INVESTIGATING THE EFFECTS OF CORROSION ON THE FATIGUE LIFE OF WELDED STEEL ATTACHMENTS

A Thesis

by

JACK WESLEY SOAPE

Submitted to the Office of Graduate Studies of
Texas A&M University
in partial fulfillment of the requirements for the degree of

MASTER OF SCIENCE

May 2012

Major Subject: Civil Engineering

Investigating the Effects of Corrosion on the Fatigue

Life of Welded Steel Attachments

INVESTIGATING THE EFFECTS OF CORROSION ON THE FATIGUE LIFE OF WELDED STEEL ATTACHMENTS

A Thesis

by

JACK WESLEY SOAPE

Submitted to the Office of Graduate Studies of
Texas A&M University
in partial fulfillment of the requirements for the degree of

MASTER OF SCIENCE

Approved by:

Chair of Committee,	Peter B. Keating
Committee Members,	Gary Fry
	Alan B. Palazzolo
Head of Department,	John Niedzwecki

May 2012

Major Subject: Civil Engineering

ABSTRACT

Investigating the Effects of Corrosion on the Fatigue

Life of Welded Steel Attachments. (May 2012)

Jack Wesley Soape, B.S., Texas A&M University

Chair of Advisory Committee: Dr. Peter B. Keating

The railroad industry plays a pivotal role in commerce and greatly impacts America's economy. With this in mind, they cannot afford downtime or service interruptions due to bridge or member replacement. Corrosion of bridges causes millions of dollars each year for the railroad industry in terms of maintenance and inspection. Since a large number of these bridges are steel and their service life is typically governed by fatigue of welded details, it is important to determine the interactions of the corrosion and fatigue mechanisms. While there are differing opinions on the effects of corrosion on the fatigue life of welded steel attachments, the intent of this research is to experimentally investigate the relationship between fatigue and corrosion and determine whether this relationship is beneficial, neutral, or detrimental to the fatigue behavior of welded attachments.

In order to investigate the effects of corrosion on the fatigue life of welded steel attachments, a testing methodology simulating the conditions a bridge could be expected to experience during its service life is established, executed and the results evaluated.

Thirty-two specimens were subjected to cycles of corrosion and interval fatigue loading at varying corrosion times and fatigue cycles. These corrosion-fatigue specimens were then compared to the five control (non-corroded) control specimens and three pre-corroded specimens.

The results show that the fatigue life of welded steel attachments is not decreased by the effects of corrosion until more than half of the cross section has been reduced. Specimens subjected to a ‘pre-corrosion’ period occurring in the absence of fatigue loading, then subjected to cyclic fatigue loading at a later time have drastically reduced fatigue lives.

TABLE OF CONTENTS

Page

Page

LIST OF FIGURES

Page

Page

Page

LIST OF TABLES

Page

1. INTRODUCTION

1.1 Background

In 2011 the railroad industry invested over $20 billion into our nation's rail network. With over 139,000 miles of railroads and nearly 170,000 employees, the railroads play a pivotal role in not only the American economy but also America's productivity (Railroad Infrastructure Investment, 2012). With stakes this high, an industry cannot afford any downtime or service interruption. By improving the inspection practices and, in turn, prolonging the service life of bridges, the industry can better allocate their financial resources to increase overall productivity.

Over the years, our nation's infrastructure has garnered a great deal of attention from the public. In 2009 the American Society of Civil Engineers (ASCE) gave the United States a grade 'D' for overall infrastructure and a 'C' for bridges (Home: Report Card for America's Infrastructure, 2011). At a cost of $2.2 trillion over a period of five years, it would require extensive resources to raise our infrastructure to an acceptable level. What if the corrosion process was not detrimental to the service life of steel bridges?

One of the primary design criteria for bridges is fatigue. Fatigue occurs when cyclical loads cause localized plastic stresses at the tip of an existing flaw or crack.

This thesis follows the style of *ASCE: Journal of Structural Engineering*.

These plastic stresses lead to deformation and damage causing the crack to grow. Abrupt changes in cross section are significant contributors to increasing the applied stress to the plastic stress zone by providing a geometric stress concentration. Fatigue design is based on the severity of the stress concentration induced by changes in cross section and the respective inherent flaws incurred during the manufacture and fabrication of each specific condition. With each load cycle the crack grows by an incremental amount which can ultimately lead to failure.

Previous research programs have tried to determine the relationship between corrosion and fatigue in steel; all of which have lead to different conclusions. Various researchers have concluded that the corrosion process decreases the fatigue life of welded details while others suggested that corrosion can extend the fatigue life.

1.2 Research Objective

The objective of this research program is to validate a testing methodology that simulates the coupling of the corrosion process with fatigue crack initiation and propagation. A better understanding of this relationship will provide bridge owners with better tools to manage the maintenance of bridges as well to operate bridges with increased reliability in their safety.

2. FATIGUE AND CORROSION DAMAGE

2.1 Fatigue

Since the 1950's, structural engineers have been trying to minimize the effects of fatigue on steel bridges. Fatigue life is always a concern during the design of a structure which will see cyclical loads over its lifespan. Fatigue damage occurs when a small flaw slowly propagates into a crack due to repeated load cycles. Although flaws are not always visible, they exist in all materials. For bridges, the governing fatigue life is typically attributed to welded sections. As Fisher et al. (1974) noted, fatigue cracks are first seen at welds and weld terminations around stiffeners, gusset plates, cover plates, or other attachments. The fatigue life for welded details is typically governed by the presence of defects (undercut, slag inclusions, shrinkage cracks, misalignment, etc.), while the surface defects prove to be the most detrimental to fatigue life. These defects reside in the stress concentration region of the weld toe and serve as locations for fatigue crack nucleation (Fisher, Frank, Hirt, & McNamee, 1970).

An initial flaw must experience tensile stresses for a fatigue crack to occur. During the welding process, regions of high residual tensile stress are created. The residual stress in these regions can be as high as the tensile yielding stress. These areas of residual tensile stress are what have caused a higher occurrence of fatigue related issues in welded construction as compared to riveted construction of the past. Since weldments have regions of high tensile residual stress, all stress cycles are fully effective

in contributing to crack propagation, even if a portion of the stress cycle is compressive. For the flaw to propagate, the cyclical load must exceed a threshold value. Below this threshold value, only elastic stresses are experienced at the crack tip, which does not result in any growth. Above this threshold level, the crack tip develops a plastic stress region, which causes deformation and leads to the crack growing with each load cycle. As the crack grows, the net section is decreased, reducing the load carrying capacity and increasing the overall stress. As the stress increases, the amount of growth occurring during each successive load cycle increases, leading to exponential growth. The different category of fatigue details (A, B, C, etc.) as recognized by AISC, AASHTO, etc., are dependent on the geometric stress risers present at a specific section.

It is very hard to determine the initial flaw size in welds by non-destructive testing methods. After the completion of fatigue testing, the initial flaw size can be determined by careful inspection using high magnification microscopes. Since the sizes can only be known after failure, researchers use various assumptions for initial flaw size in order to calculate a projected fatigue life. Barsom (1984) found that for category C, D, and E details the flaws were “equal to or smaller than 0.016 in.” Sakano et al. (1989) later assumed an initial depth of 20μm (0.000787 in) for estimating the fatigue life.

Although initial flaws may exist, they do not immediately begin to propagate as a crack with the first cycle experienced. The initial flaws do not contain sharp crack tips required for crack propagation to occur. Fatigue life is composed of two segments: crack initiation and crack propagation. For high-cycle fatigue lives, the crack initiation phase is predominant. The initiation phase is required to transform the radiused root of the

initial defect into a sharp crack-like flaw. Numerous researchers have concluded that approximately 80% of the fatigue life of low stress-high cycle specimens are attributed to crack initiation.

2.2 Corrosion

ASM (2003) defines aqueous corrosion as "an electrochemical process occurring at the interface between a material and an aqueous solution." For this to happen, an oxidation and reduction (redox) reaction occur at the same time.

The oxidation reaction is the dissolution of the metal and or the formation of metal oxide, while the reduction reaction is dissolved oxygen reduction. The redox reaction of iron can be seen in the following equation (ASM, 2003):

$$2Fe + O_2 + 2H_2O \rightarrow 2Fe^{2+} + 4OH^-$$

When the dissolved oxygen in the saltwater reacts with the metallic iron in steel, the iron is converted to rust. This reaction leads to the iron anode being 'eaten away' as the rust deposit grows (Fisher, Yen, & Wang, 1991). Pitting occurs when a passive film, such as mill scale, suffers a localized breakdown. This breakdown creates an anode, and leads to the accelerated dissolution of the underlying metal (ASM, 2003). Figure 1 shows a deposit of corrosion product around a weld toe due to corrosion in an aqueous environment.

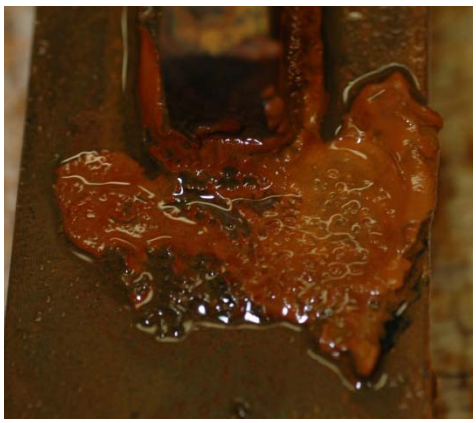

Figure 1. Corrosion Product Deposit

During the fabrication and construction phase of a bridge, the steel is either sandblasted to remove mill scale then painted, or in the case of weathering steel, the mill scale is removed to allow for 'uniform' weathering. Both of these methods are done in an attempt of corrosion protection. During the life cycle of a bridge, the initial paint coating will slowly deteriorate and form cracks. If the mill scale is left on, it will also develop cracks under loading due to its brittle nature. Neither method of surface treatment is completely successful at mitigating the effects of corrosion.

Similar to fatigue cracks, the corrosion process begins at the surface. Cracks in the mill scale or paint coating form optimal environments for crevice corrosion and pitting to take place (Albrecht & Friedland, 1980; Fisher, Kaufmann, & Pense, 1998). In carbon steel and high-strength low-alloy steel these small surface cracks in the protective layer (paint or mill scale) lead to an accelerated corrosion rate as compared to a nearby

flat area of steel (Fisher, Yen, & Wang, 1991). Even in weathering steels (e.g., ASTM A588), which are expected to form a protective coating under optimal weathering conditions, these surface flaws lead to localized pitting as it provides an oxygen deficient region which acts as the anode for an active corrosion cell (Fisher, Yen, & Wang, 1991). Since mill scale is cathodic, it is complementary to the anodic region, completing the corrosion cell (Culp & Tinklenberg, 1980). Since abrupt changes in geometry, such as a cover plate termination, not only provide a region of stress concentration but can also make it difficult to apply a protective coating, like paint, these areas tend to show the first signs of corrosion.

During the welding process the mill scale's integrity is compromised, due to the high heat, after which it can easily flake off. As the corrosion mechanism continues, the affected area will grow outward from the weld. Over time as the corrosion spreads, it reduces the material thickness as the rust scale flakes away (Culp & Tinklenberg, 1980). Figure 2 shows the process of corrosion as it spreads from the toe of a weld. The small crater-like areas seen are individual corrosion cells where the 'pit' of the crater is the local anode.

Figure 2. Surface Corrosion Around Weld

Figure 3 shows the effects of corrosion on an unpainted mill scale surface after 15 corrosion cycles of 7 days each in a 3.5% NaCl solution. The areas of bare steel are where the corrosion process has begun. On the left is a stiffener plate and its weld toe. The weld toe was the first area to corrode and then began to progress outward. At the same time, small surface imperfections in the mill scale, which occurred during the rolling process, begin to corrode. On the far right is the grip section of the specimen. The tensile grips use a cross hatch pattern to grip the steel which causes breaks in the mill scale. Figure 4 is a more advanced case of corrosion of mill scale than that of Figure 3.

Figure 3. Initial Corrosion of Mill Scale

Figure 4. Advanced Corrosion of Mill Scale

2.3 Applications

Initially, weathering steel was used in bridges because early laboratory testing showed that under regular wet/dry cycles the high copper content would allow the formation of a dense outer oxide which would resist future corrosion. In the 1970's the Michigan Department of Transportation conducted a study on the effects of corrosion on weathering steel. Weathering steel had started becoming more prevalent in cases where

the bridge would be located over a roadway with high volume traffic below. Due to the required regular painting of low-alloy steel bridges, it was decided that the additional initial cost of weathering steel would be more economical than the prohibitive costs of traffic control associated with the maintenance associated with traditional low-alloy structural steel (Culp & Tinklenberg, 1980).

It was found that in bridge applications weathering steel was not performing as expected. Due to Michigan being in a northern climate, deicing salts were used during the winter months. When weathering steel is contaminated with these salts, the steel corrodes in the same fashion as traditional non-weathering steels. The salt penetrates the dense protective oxide and corrodes the material beneath, which forces the protective oxide layer to rupture as the corrosion product underneath it expands. Initially, the ends of the bridge girders, which came into contact with supports, were painted in an attempt to prevent contact with the deicing salts. Upon inspection, it was realized that the middle section of the bridge girders were exposed to salt contaminated water runoff through holes in the bridge deck and leaking expansion joints (Culp & Tinklenberg, 1980).

Bridges with and without under-bridge traffic were also subject to airborne salt contamination. When deicing salts were applied to the roadways, the vehicle traffic would create a ‘salt cloud,’ which would then settle on the bridge structure. This occurred regardless of if the bridge structure was above or below the roadway. This airborne salt contamination even occurred on river crossing bridges (Culp & Tinklenberg, 1980).

Salt contamination was not the sole reason that weathering steels were exceeding expected corrosion rates. Girder details, such as stiffeners, become catch-alls for dirt and debris. Upon closer inspection, it was realized that this debris maintained a moist environment, extending the time of wetness (TOW), which led to extensive corrosion damage and localized pitting around the detail (Culp & Tinklenberg, 1980).

Since weathering steels are proven to behave comparably to low-alloy steel in the field, any research regarding the corrosion-fatigue performance of low-alloy steel can be extrapolated and applied to weathering steels without the need to consider two separate steel types.

2.4 Previous Research

Throughout the years many well intentioned testing theories have been executed in attempt to understand the correlation between corrosion and fatigue life. The effects of corrosion on fatigue life are of importance to many facets of the engineering community; although there are two sectors from which most of the previous research was generated: bridge and offshore structures. Unfortunately, none of these testing theories has recreated an accurate representation of the service conditions bridges experience.

Albrecht et al. (1983; 1980) conducted a study on small samples and concluded that if weathering steel were left to weather over a long period of time, the micro-cracks in the mill scale would lead to crevice corrosion and early crack nucleation. The test

specimens were composed of ASTM A588 weathering steel with two welded transverse stiffeners, which created a Category C detail. The experiment used six stress ranges: 110 MPa, 124 MPa, 144 MPa, 177 MPa, 229 MPa, and 262 MPa (16.0 ksi, 18.0 ksi, 20.9 ksi, 25.6 ksi, 33.2 ksi, and 38.0 ksi). A minimum stress of 3 MPa (0.5 ksi) was used for all six stress ranges. From a total of 62 specimens, 12 were tested in as-welded condition, 16 were tested after three years of weathering, and 22 were tested after eight years of weathering. The remaining 12 specimens were weathered for three years, tested to one-eighth of the average life of the previously tested 3 year weathered specimens, then weathered for another six months. At the end of six month weathering period, the specimens were again tested to one-eighth of the average 3 year specimen life. This cycle of alternate weathering and testing continued until failure.

Testing was conducted on an MTS 89 kN (20 kip) load frame using flat-plate friction grips. The load was applied as a sinusoidal wave at frequencies ranging from 5 Hz to 10 Hz with a loading rate of 668 kN/sec (150 kip/sec). Albrecht defined failure as the separation of the sample into two separate pieces.

The specimens were weathered outdoors in University Park, Maryland. Due to University Park's proximity to a large metropolitan area, the specimens were exposed to an above average amount of automobile exhaust. Although the specimens were not subjected to direct salt contamination or prolonged wet/dry cycles, rust pitting still occurred. These specimens were tested after three and eight years of weathering and it was found that they had a reduced fatigue life when compared to the control specimens.

The resulting data can be seen in Figure 5 (Albrecht & Friedland, 1980; Albrecht & Cheng, 1983).

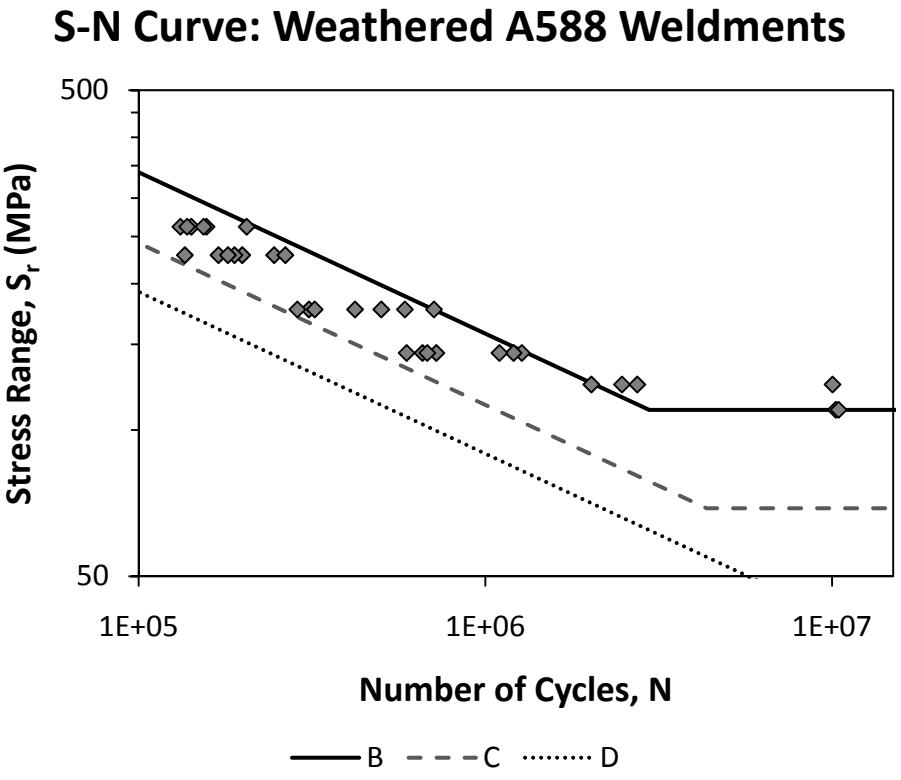

Figure 5. Weathered A588 Weldments

In another study, Albrecht et al. (1994; 2009) conducted an experiment using full size A588 beams. The beams were blast-cleaned and weathered outdoors. The beams were weathered in two different fashions, bold exposure and sheltered. During the weathering process, they were sprayed with a 3% saltwater solution, three times weekly,

during 3 months of each winter season to simulate contamination by de-icing salts. During the remainder of the weathering time, the beams were sprayed with plain water once every 2 weeks.

Three types of beams were tested: built-up welded beams, hot rolled beams, and hot rolled beams with welded cover plates. Also, three testing environments were used: air, moist freshwater and moist saltwater. The freshwater and saltwater environments were applied by using sponges, saturated with their respective solution, during the testing period. The saltwater solution was composed of 3% sodium chloride dissolved in freshwater. Failure was defined when at least 50% of the tension flange cracked (Albrecht & Shabshab, 1994; Albrecht & Lenwari, 2009).

Albrecht found that the corrosion process reduced the fatigue life of welded beams, cover-plated beams and hot rolled beams. The results of the hot rolled beam fatigue testing can be seen in Figure 6. In the sheltered, welded beams, all the cracks were observed to initiate from rust pits. These results are similar to those of the smaller weldment samples he tested previously. Since the crevice corrosion and pitting had already reduced the cross section area, prior to fatigue loading, the results are understandable (Albrecht & Shabshab, 1994; Albrecht & Lenwari, 2009).

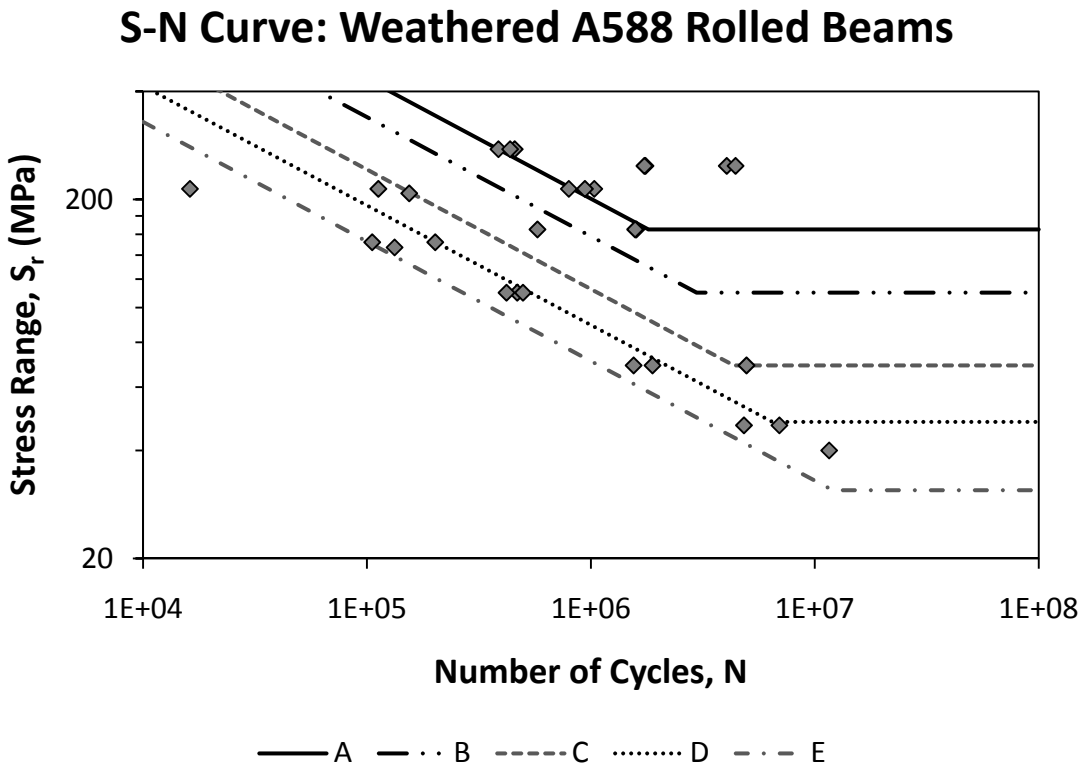

Figure 6. Weathered A588 Rolled Beams

Vaessen et al. (1982) and van Leeuwen et al. (1980) developed a similar conclusion to Albrecht regarding the relationship between corrosion and fatigue life. They conducted an experiment using constant amplitude fatigue tests on BS 4360 Grade D steel specimens with one welded transverse stiffener. Testing was carried out in two environments: air and seawater. The specimens were tested under four-point bending in either an MTS or Schenck testing system. The constant amplitude load was applied as a sinusoidal wave at a frequency between 2 Hz to 5 Hz for the specimens tested in air, and at 0.2 Hz for the specimens tested in seawater. Similar to Albrecht's early experiments,

all cracks initiated from locations near the toe of the weld. Vaessen and van Leeuwen found that the existing design curves were not accurate for projecting the fatigue lives of welded joints experiencing corrosion by immersion in a seawater environment.

Palin-Luc et al. (2010) conducted testing on low-alloy steel specimens. These findings also supported those previously found by Albrecht. The test specimens were made of non-standard hot rolled low-alloy steel, typically used in the manufacture of mooring chains. Testing was conducted at 20 kHz on an ultrasonic fatigue testing machine. Three conditions were tested: without corrosion, after pre-corrosion and under real time artificial seawater flow.

Palin-Luc et al. found that for non-corroded specimens, fatigue cracks propagated from surface flaws. For the pre-corroded specimens and specimens tested while immersed, failure occurred due to fatigue cracks propagating from surface corrosion pits (Palin-Luc, Perez-Mora, Bathias, Dominguez, Paris, & Arana, 2010).

Both Barsom (1984), Out et al. (1984), and Fisher et al. (1991) have proposed that the corrosion process can be beneficial to the fatigue life. Due to the critical flaws responsible for fatigue failure of welded details being located on the surface, the controlling fatigue life is greatly influenced by the stress concentrations welding typically creates. If the environmental corrosion rate is higher than the crack propagation rate, the corrosion process could “eliminate or at least decrease the size of the surface imperfections.” By reducing the flaw size, corrosion would in turn reduce the stress raiser and prolong the fatigue life (Barsom, 1984).

Out et al. (1984) conducted testing on four built-up riveted stringers taken from a railroad bridge. The bridge from which the stringers originated was 80 years old, and had considerable signs of corrosion damage. The purpose of the experiment was to determine the fatigue life of riveted details in high-cycle regions, and determine the fatigue behavior of built-up members that suffered deterioration, due to corrosion, during service. The stringers were tested using two Amsler 245 kN (55 kip) hydraulic jacks and one pulsator in a four-point bending arrangement. The load was applied at a constant amplitude of 520 cycles per minute (8.67 Hz). Out concluded that if the net cross section was reduced by more than half due to corrosion, the resulting fatigue life was more accurately predicted by the next severe detail category. (For example, for the category D sections that had lost more than half of their area to corrosion, their fatigue life was more accurately predicted by the design life of category E.)

Waldvogel (1997) conducted testing on the effects of corrosion on the fatigue life of steel specimens with a machined notch. The specimens were machined into a dog-bone shape with a $1/32^{nd}$ of an inch (0.8 mm) groove perpendicular to the direction of loading. Testing was conducted on an MTS load frame with a nominal stress range of 35 ksi (241.3 MPa) applied as a sinusoidal wave at 20 Hz. Corrosion took place in a 3.5% sodium chloride solution for a period of either 3.5 days or 7 days, depending on which exposure group the specimen belonged to. The incremental fatigue loading cycles, of each load group, were based on 50%, 25%, 12.5% or 6.25% of the average control specimen fatigue life.

After an initial exposure period of seven days for all specimens in the sodium chloride solution, the specimens were then subjected to their respective incremental fatigue loading cycles. After the incremental fatigue loading, specimens were returned to the corrosion solution for another exposure period of either 3.5 days or 7 days. This sequence of alternating exposure to a corrosive environment and incremental fatigue loading continued until the specimen failed due to unstable fatigue crack growth. Failure was defined as the specimen separating into two separate pieces due to fatigue crack propagation. After each exposure period in the corrosion solution, specimens were cleaned prior to the incremental fatigue loading. This cleaning process removed the corrosion product, and allowed for more thickness measurements to be taken, in order to record the corrosion rate.

Although the data showed that the mean corroded fatigue life exceeded the mean non-corroded fatigue life, due to the high fatigue cycle intervals which the specimens experienced, the results were inconclusive in showing a delay in the crack initiation due to corrosion (Waldvogel, 1997).

The research conducted by Ewalds and Edwards (1982) discussing the effects of crack closure prevention due to corrosion product wedging, should also be addressed. The wedging of corrosion product causes a raise in the minimum stress intensity factor. This change results in the total range of the stress intensity factor, which is the driving force determining crack growth rates, is decreased. If the stress range intensity factor is decreased sufficiently, the result can be retardation or even stopping the crack growth.

While this phenomena is possible on notched specimens fatigue tested while submersed in a corrosive solution, this will not occur in the welded details previously discussed. By testing while the specimen is submersed, it allows for the pumping effect of the crack displacement to introduce the corrosive solution to the entire depth of the crack. This does not occur during typical bridge loading as the bridge members are not submerged and the corrosion occurs on the surface. Without the pumping effect, the corrosion product cannot develop within the crack, and in turn cause corrosion product wedging.

Also, welded sections typical to bridges have regions of high residual tensile stress in the area where the fatigue crack is expected to occur. This region of high residual tensile stress raises the effective stress range the crack experiences. As the range of effective stress is raised, the minimum stress value is above the level which could be affected by corrosion product being present within the crack. Since the crack does not close due to the residual tensile stresses, the findings of Ewalds and Edwards (1982) is interesting, but not directly applicable to this research.

2.5 Objective

The objective of this research is to show that the corrosion process is not detrimental to the fatigue life in most cases. Since both the corrosion process and critical fatigue cracks begin on the surface, it seems logical to deduce that corrosion could in fact be beneficial to fatigue life. Based on the relationships shown in Figure 7, it can be

reasoned that if the environment was sufficiently corrosive, such that the corrosion mechanism could 'eat away' at the initial flaw, and decrease the flaw size, or remove the flaw altogether, the fatigue life could be increased, if not extended.

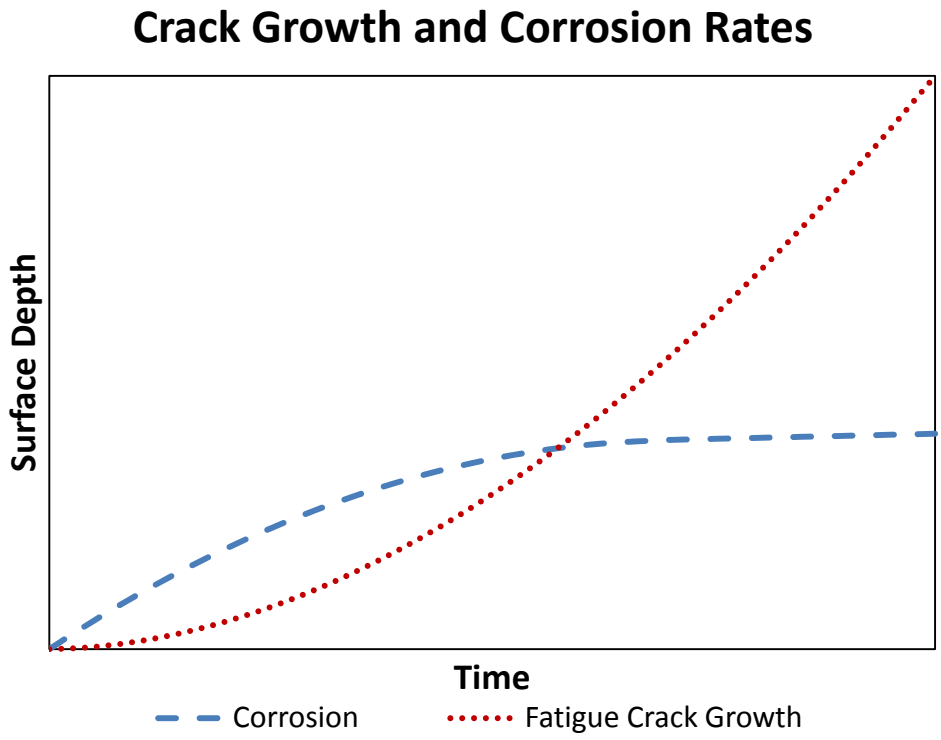

Figure 7. Qualitative Diagram of Crack Growth and Corrosion Rate vs. Time

Figure 7 is based on generalized qualitative rates a bridge could be expected to experience during service. Based on local conditions which could greatly influence the individual corrosion and fatigue growth rates, this example is only used to express their relative behaviors in reference to each other. Excessive or long-term corrosion could

result in significant cross section loss causing fracture, or yielding in the event of overload. This hypothesis is also supported by Fisher et al. (1991) during his field investigation of riveted bridge members, as well as by Barsom (1984).

The hypothesis that corrosion does not accelerate fatigue crack growth is based on fracture mechanics. For a fillet weld toe, fatigue failure occurs when surface flaws develop into unstable cracks. If the corrosion process can slow the development of these flaws, the fatigue life could be extended.

To test this hypothesis in a laboratory, the typical bridge service life must be condensed into a reasonable period of time. Although there have previously been studies conducted on weathering steels (ASTM A588), the current research intends to determine the effects that corrosion has on the fatigue life of low-alloy structural steel, since the findings can be applied to weathering steel subject to corrosion due to non-optimal service environments.

3. TESTING PARAMETERS & PROCEDURE

To investigate the effects of corrosion on the fatigue life, the corrosion specimens were subjected to alternating periods of exposure to a corrosive environment and cyclic fatigue loading.

The specimens consisted of a 51mm x 3mm x 381mm (2” x 1/8” x 15”) long main plate, to which one 25.5mm x 13mm x 127mm (1” x 1/2” x 5”) longitudinal stiffener was welded to each side with a 5mm (3/16”) weld. Since the tensile strength has no relation to the fatigue life, all specimens were created from ASTM A36 bar stock (Fisher, Frank, Hirt, & McNamee, 1970; Fisher, Albrecht, & Yen, 1974). The welds were made using a MIG welder with AWS 5.18 ER70S-6 wire. All specimens were fabricated on the same day by one professional welder to ensure consistency. A typical weld toe where fatigue cracks are expected to propagate from can be seen in Figure 8. The dimensions and configuration of the specimens can be seen in Figure 9.

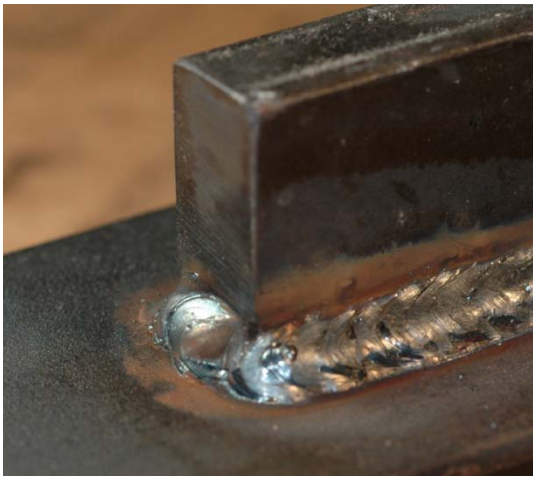

Figure 8. Typical Weld Toe

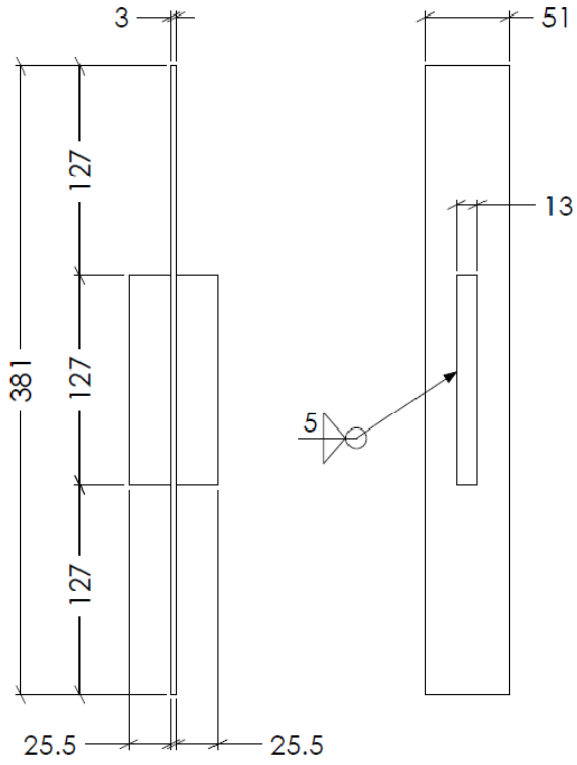

Figure 9. Fatigue Specimen Geometry

This AASHTO Category E detail was chosen to provide a lower nominal stress range, similar to what railroad bridges experience in service, while still having a reasonably short life cycle. If the nominal stress were, lower it would greatly increase the fatigue life, and extend the research beyond a reasonable time frame.

All specimens were tested with a stress range (S_r) of 138 MPa (20 ksi), and a minimum stress (S_{min}) of 69 MPa (10 ksi). The loading was applied at 30 Hz as a constant amplitude sinusoidal wave. This loading rate was chosen due to the low stress range, which would cause a high cycle fatigue life. Had the loading rate been lower, each testing sequence would have extended beyond a reasonable time frame. Additionally, the specimens were preloaded to a mean stress of 138 MPa (20 ksi) to begin testing. The preload was applied to prevent the process variable control (PVC) function of the testing software from exceeding the maximum stress value during the first quarter of the sine wave as the load ramps upwards. The servo-hydraulic test frame used was an MTS Model 312.21, capable of producing 100 kN (22 kips) of force. The servo-hydraulic test frame was controlled by MTS Basic TestWare software program. The software was used in its load control mode, which allowed the user to determine the upper and lower bounds of the sinusoidal load wave. In addition to the applied load function settings, force and displacement interlocks were utilized to ensure that power surges or shortages did not influence the results. Since the program was in load control, the only data that needed to be recorded was cycle count, which was recorded in the test log. Each specimen had a designated testing and log file that kept a continuous record of each individual incremental fatigue loading cycle counts, total fatigue cycle counts to

date, and any errors encountered (such as the displacement/force interlocks being tripped). Figure 10 shows a specimen in the MTS load frame during testing.

Figure 10. Specimen in Test Frame

Due to the number of specimens involved, three 6m (20’) sections of bar stock were used for the base metal. From each of the three sections, material was tested in tension to determine the individual yield and ultimate strengths, as well as having its chemistry content analyzed. The results are shown in Figure 11 and Table 1, respectively.

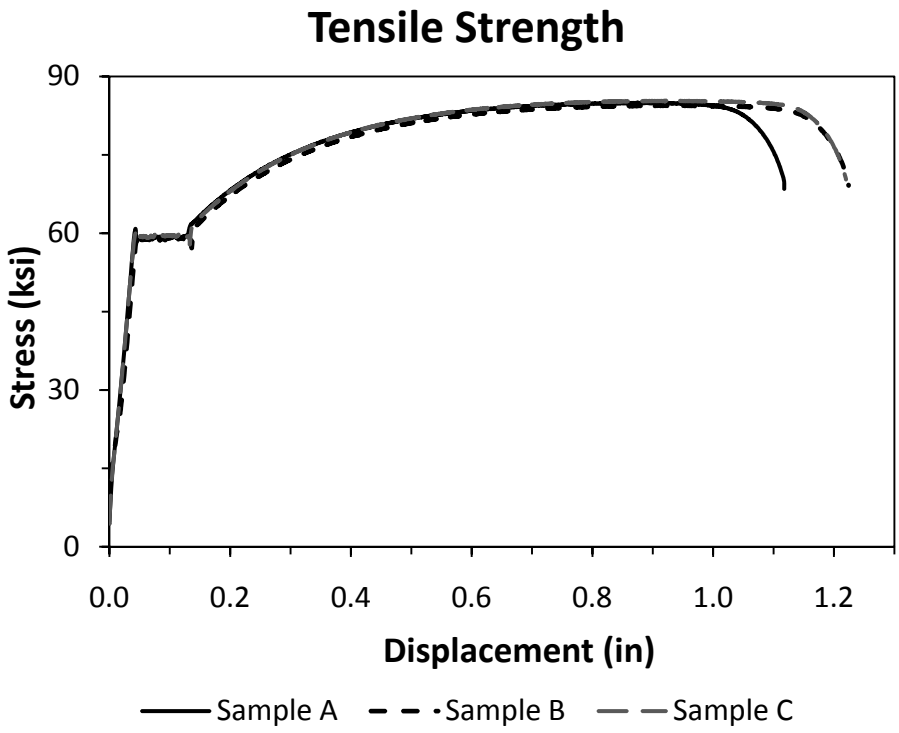

Figure 11. Tensile Test Results

Table 1. Steel Chemistry and Strength Test Results

Sample:	A	B	C	Weld	A36
Carbon	0.2	0.2	0.2	0.091	0.25 (max)
Manganese	0.8	0.77	0.77	1.13	
Phosphorus	0.045	0.046	0.046	0.029	0.04 (max)
Sulfur	0.047	0.033	0.034	0.033	0.05 (max)
Silicon	0.18	0.15	0.15	0.61	0.40 (max)
Nickel	0.13	0.12	0.12	0.03	
Molybdenum	0.02	0.02	0.02	0.01	
Chromium	0.09	0.09	0.09	0.04	
Copper	0.56	0.56	0.56	0.36	0.20 (min)
Cobalt	0.011	0.011	0.011	0.005	
Tin	0.020	0.018	0.018	<0.005	
F_y (ksi)	61	60	60		36 (min)
F_u (ksi)	85	84.5	85		36 (min)

Figure 11 shows that each of the three samples had very similar behavior during the yield and ultimate strength testing. Based on the similarity of the stress-strain plots of 'Sample B' and 'Sample C', it is likely that both came from the same stock. While 'Sample A' had slightly less elongation prior to failure than the other two samples, all yield strengths and ultimate strengths are nearly identical. The high yield strength results of these samples are typical of thin A36 steel plate.

The samples also had very similar chemical content, which can be seen in Table 1. It is obvious that the chemical content meets the minimum ASTM requirements for A36 steel. It should also be noted that the chemical composition is very similar to the requirements for weathering steel (A588). Because of this chemical similarity to weathering steel, the conclusions of this research will be applicable to both weathering

and non-weathering steels alike. The consistency of these three samples is beneficial for this experiment since there are no major variances in the strength or chemical composition. This consistency allows for a more controlled experiment with less factors of uncertainty.

Five control specimens were fatigue tested without exposure to a corrosive environment in order to establish a baseline for the fatigue life. For both the control and corrosion specimens, failure was defined as the separation of the specimen into two separate pieces. The results of the control specimen fatigue lives are shown in Table 2, and plotted with the lower bound design life for AASHTO Category E details in Figure 12.

Table 2. Control Specimen Fatigue Life

Specimen	Base Metal	Fatigue Life
CS I	A	645,244
CS II	B	687,437
CS III	C	362,802
CS IV	C	445,190
CS V	A	448,703
Average Life :		**518,000**

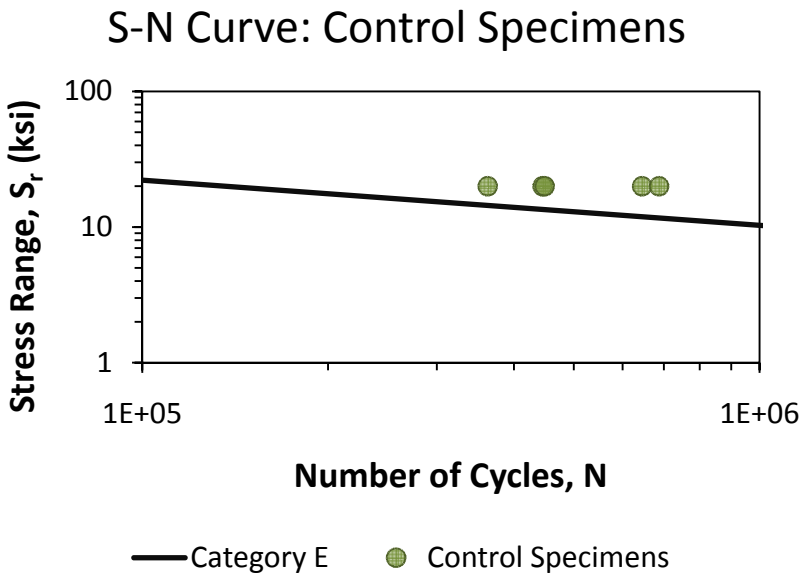

Figure 12. S-N Curve for Control Specimens

Although the results have a relatively large range, these fatigue lives represent the scatter associated with welded joints. It should also be noted that all of the control specimens had a fatigue life that exceeded the lower bound design life for Category E welded details.

Once a baseline average fatigue life for non-corroded welded attachments was established, four intervals of fatigue cycle loading were selected. There were thirty-two corrosion-fatigue specimens divided into two groups of sixteen each. Both groups of sixteen specimens experienced a different time interval for exposure to a corrosive environment. One exposure group was exposed for seven days, and the second group for three and one half days. These two exposure groups will be referred to as the '7 Day' and the '3.5 Day' groups, respectively.

Each exposure group was tested at the end of its exposure period; after the incremental fatigue testing, the surviving specimens within the exposure group were returned to the corrosive environment for their respective exposure times. Prior to each fatigue testing interval, specimens were individually cleaned under running water with a nylon brush and steel wool to remove any corrosion scale that had accumulated during the exposure period. As a result of this cleaning process, the corrosion rate was a linear function of time, which closely approximates the long-term steady-state corrosion of bridges. The corrosion process and fatigue loading sequence was repeated until failure.

Each of the two exposure groups were further divided into four groups of four. These sub-groups would each experience separate fatigue load cycle intervals at the end of each exposure period. The four fatigue load cycle intervals were determined as a percentage of the average control specimen fatigue lives (Table 2). Each sub-group's incremental fatigue cycle count is shown in Table 3.

Table 3. Fatigue Cycle Intervals

Percentage of Control Life	Cycles	Testing Intervals to Reach Design Life	Testing Intervals to Reach Mean Control Life
5.0%	26,000	6	20
2.5%	13,000	11	40
1.0%	5,200	27	100
0.5%	2,600	53	200

From Table 3, it can be seen that the specimen group projected to reach mean control life first is the 5%-‘3.5 Day’ after 10 weeks, and the last group will be the 0.5%-‘7 Day’ after 200 weeks.

To ensure that accurate records were kept, all corrosion-fatigue specimens were marked on the face of the longitudinal stiffener with steel stamps. A diagram of these marking is shown in Figure 13. The first numbers (2.5-1) denote the percentage of average control fatigue life per test interval and the individual specimen number, which ranged from 1-4. The middle number identifies the time interval of exposure to the corrosive environment, whether it is seven days, or in this example, three and a half. The final letter identifies the main base plate metal, A, B, or C. A picture of one end of a specimen can be seen in Figure 14.

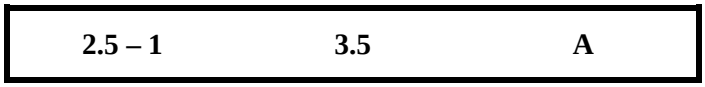

Figure 13. Specimen Identification

Figure 14. Stamped Specimen

In addition to the corrosion-fatigue specimens, there were three pre-corroded specimens. These three specimens were placed into the corrosion solution and did not experience any interval fatigue loading. The pre-corroded specimens were marked as 'X-1','X-2', and 'X-3'. To maintain similar conditions as the corrosion-fatigue specimens, the pre-corroded specimens were removed from the corrosion bath and cleaned every seven days. The pre-corroded specimens were to determine the effect on the fatigue life of specimens suffering from corrosion cross section loss prior to any cyclic fatigue loading, similar to the experiments performed by Albrecht (1984).

The corrosion-fatigue specimens were initially placed in the corrosive environment for seven days prior to the start of the fatigue loading intervals. After this initial exposure period, each specimen was subjected to its respective fatigue loading interval, then returned to the corrosive environment for another exposure period (3.5 days or 7 days).

The corrosive environment, that the corrosion-fatigue and pre-corroded specimens were exposed to, was composed of eight containers which housed the

specimens. The containers were supplied with a corrosion solution of 3.5% NaCl dissolved in water from a 100 gallon poly tank reservoir at a refresh rate of approximately 45 minutes. There were four air pumps to ensure that the corrosion solution was continuously saturated with air. Two air pumps were located by the reservoir tank, while the other two air pumps, each having four air outlets, allowed for one airstone to be placed into each corrosion container. Since the kinematics of the corrosion redox reaction are strongly influenced by temperature, two aquarium heaters were utilized to maintain a constant temperature of the corrosion solution. This was necessary since the air temperature where the corrosion bath was located fluctuated based on the time of year. Due to evaporation, the salinity level was checked at least twice a week, and adjusted accordingly to maintain a constant 3.5%. The corrosion solution was also changed at the beginning of each month to prevent saturation of iron ions which could slow down or possibly stop the corrosion process.

This corrosion bath system ensured that all specimens were subjected to identical environmental conditions. The front of the corrosion bath system can be seen in Figure 15, where the water flows into the bottom of each container. Figure 16 shows the rear of the containers, where the water exits thru the two ports located near the top.

Figure 15. Front of Corrosion Containers

Figure 16. Back of Corrosion Containers

4. RESULTS AND DISCUSSION

4.1 Fatigue Life

While the test is still on-going, these are the results from each corrosion-fatigue group whose entire specimen population has failed to date. The fatigue lives of the corrosion-fatigue specimens are show below in Table 4 and Table 5. The corresponding S-N plots can be seen in Figure 17 - Figure 22. In the S-N plots, the results from each respective testing group are shown along with the AASHTO design curve for Category E welded attachments. This fatigue design curve provides a lower bound fatigue life of 137,500 cycles at a stress range of 20 ksi.

Table 4. '7 Day' Corrosion-Fatigue Specimens

Specimen	Total Cycles
5 - 1	392,438
5 - 2	365,208
5 - 3	558,968
5 - 4	802,714
Average :	**530,000**
2.5 - 1	481,620
2.5 - 2	525,917
2.5 - 3	617,495
2.5 - 4	673,790
Average :	**575,000**

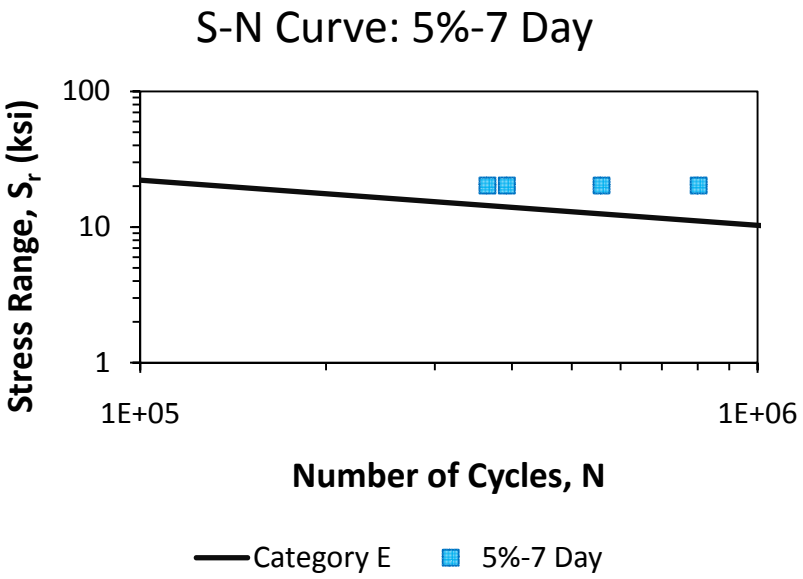

Figure 17. S-N Curve for 5%-7 Day Specimens

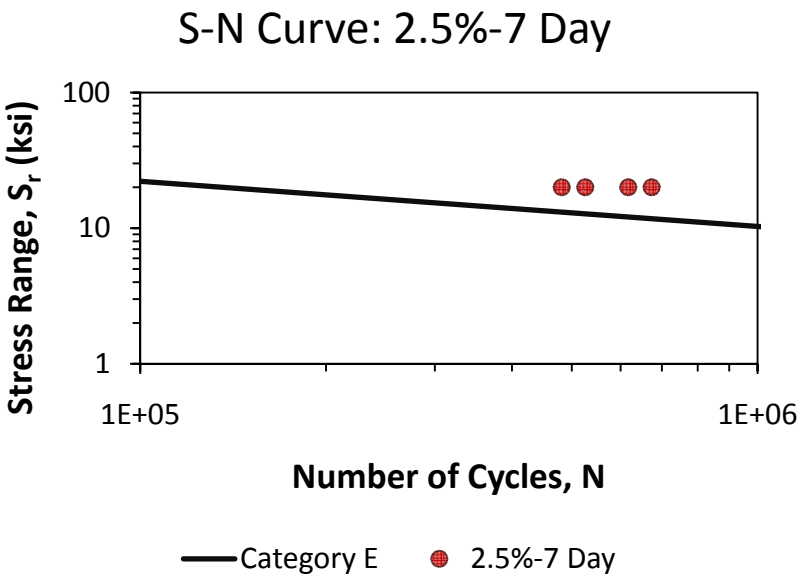

Figure 18. S-N Curve for 2.5%-7 Day Specimens

Table 5. '3.5 Day' Corrosion-Fatigue Specimens

Specimens	Total Cycles
5 - 1	344,401
5 - 2	256,249
5 - 3	476,219
5 - 4	1,325,020
Average :	**600,000**
2.5 - 1	338,490
2.5 - 2	637,072
2.5 - 3	662,612
2.5 - 4	617,362
Average :	**564,000**
1 - 1	444,973
1 - 2	449,427
1 - 3	398,991
1 - 4	397,405
Average :	**423,000**
0.5 - 1	202,684
0.5 - 2	215,595
0.5 - 3	201,714
0.5 - 4	207,978
Average :	**207,000**

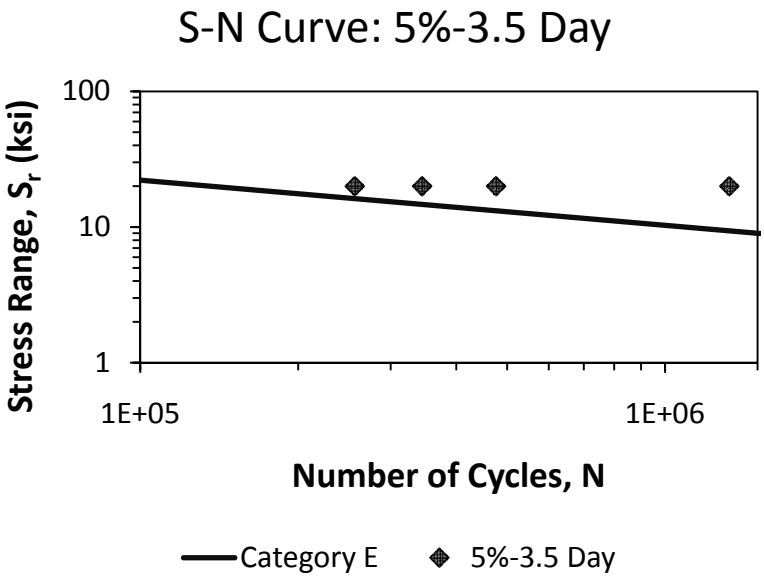

Figure 19. S-N Curve for 5%-3.5 Day Specimens

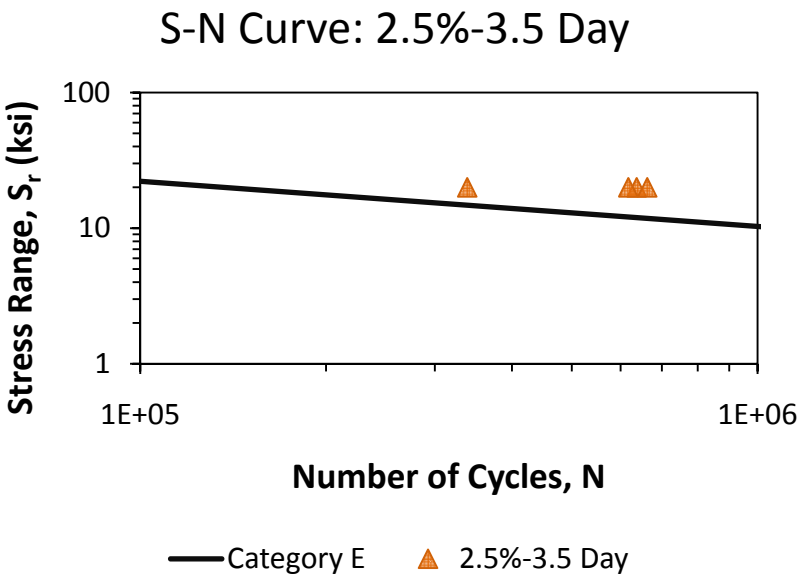

Figure 20. S-N Curve for 2.5%-3.5 Day Specimens

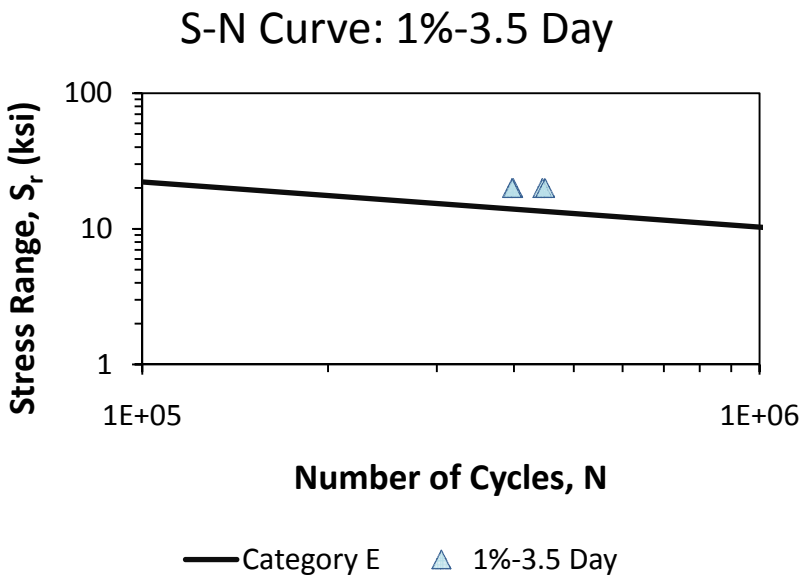

Figure 21. S-N Curve for 1%-3.5 Day Specimens

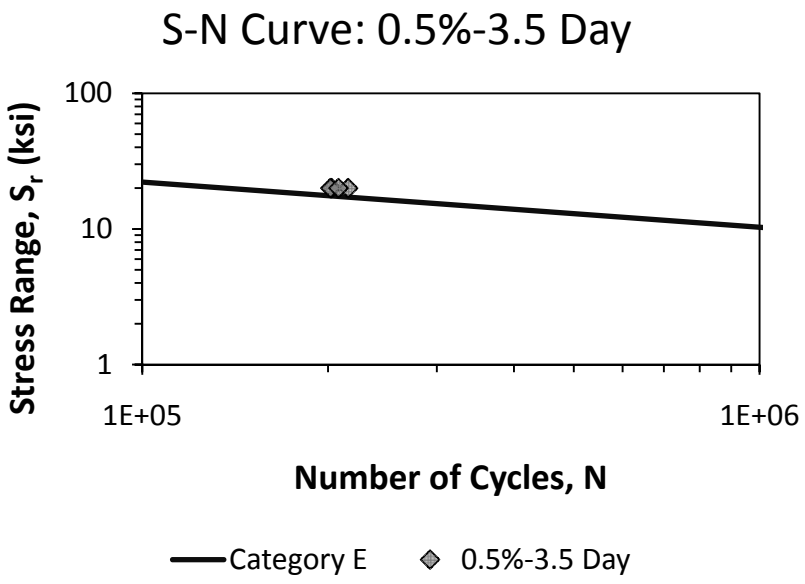

Figure 22. S-N Curve for 0.5%-3.5 Day Specimens

As seen in Table 5, the fatigue lives of the corrosion-fatigue specimens in groups ‘1%-3.5 Day’ and ‘0.5%-3.5 Day’ showed a decreased fatigue life. This is likely due to the extent of corrosion damage and the resulting cross section loss. The results are discussed later in more detail.

Figure 23 shows the fatigue lives of all the previously mentioned corrosion-fatigue specimen groups with a slight vertical exaggeration for increased clarity.

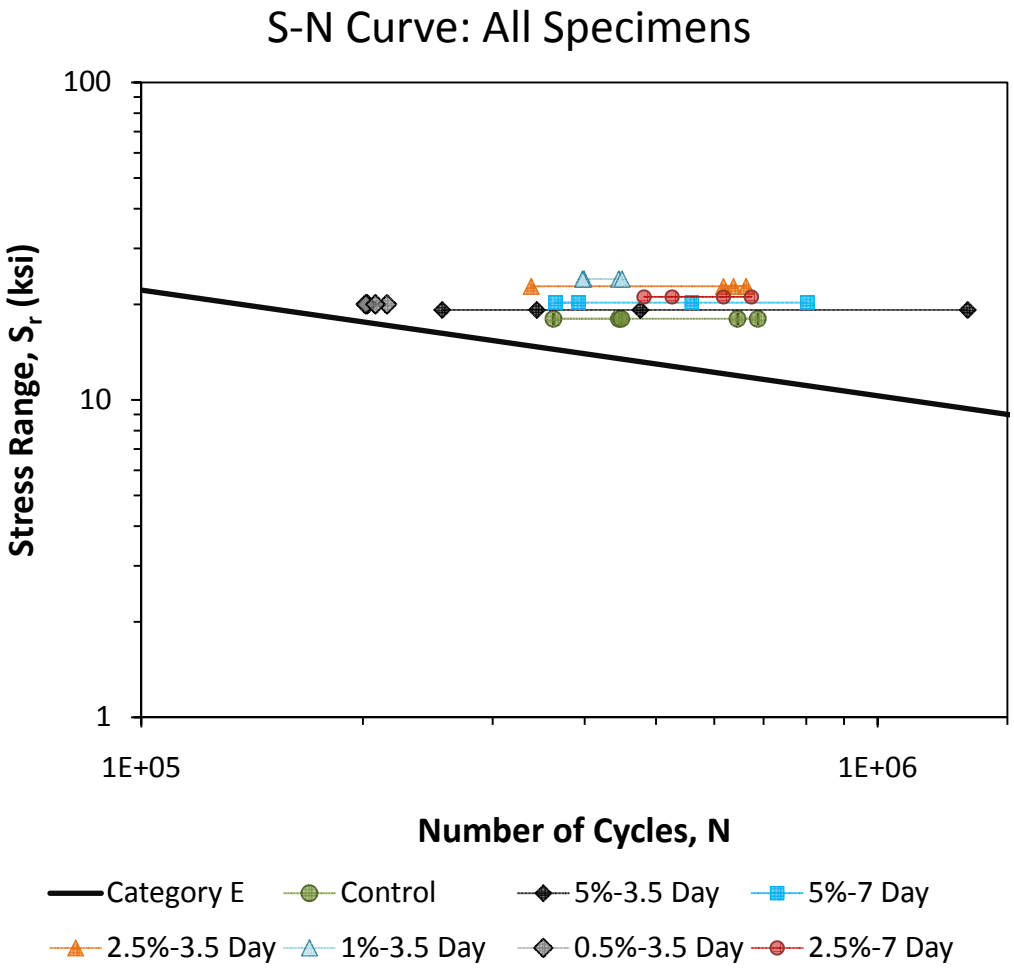

Figure 23. S-N Curve for All Corrosion-Fatigue Specimens

Below, in Figure 24 and Figure 25 a thru crack can be seen in the end of specimen '2.5-1' of the '3.5 Day' exposure group, which would ultimately lead to failure. It is evident that the fatigue crack initiated at the toe of the weld on one side and propagated until it reached a critical length. Around the edges of the following figures, the remaining mill scale can be seen. This is because the corrosion process began at the area near the weld and progressed outward in a radial fashion.

Figure 24. Thru Crack in Specimen 2.5-1 ‘3.5 Day’ (front)

Figure 25. Thru Crack in Specimen 2.5-1 ‘3.5 Day’ (back)

Figure 26 shows the fatigue fracture surface of the failure end of specimen ‘5-3’ of the ‘3.5 Day’ exposure group. It is a clear example of the incremental damage that each later fatigue loading interval contributed to the ultimate failure of the specimen. There are multiple crack initiation sites which can be seen.

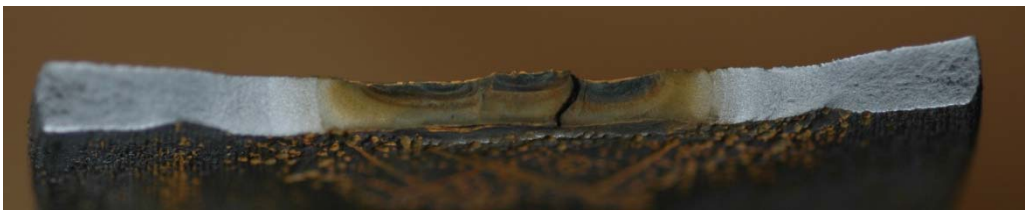

Figure 26. Fracture Surface of Specimen 5-3 ‘3.5 Day’ at ‘Failure’

While the specimens can only fail at one end of the welded stiffener, it is very likely that the remaining weld toe also experienced fatigue crack growth. To investigate, the remaining weld toe is cut down to size and the base plate is notched along the same plane as the leading edge of the weld toe. Liquid nitrogen is then used to lower the sample below its brittle transition temperature, making it easier to fracture the steel along the failure plane of the crack and the notch. The results of using this technique can be seen below in Figure 27.

Figure 27. Fracture Surface of Specimen 5-3 ‘3.5 Day’ at ‘Remaining’

4.2 Corrosion Rate

The ISO (1992) corrosion categories for steel corrosion rates can be seen in Table 6. The categories are derived from a lengthy study over a broad spectrum of environments and locations. The controlling factors of the atmospheric corrosion categories are the rate of deposition of contaminants, such as chloride ions, onto a surface and the time of wetness (TOW). While individual metals have different corrosion rates in each category, these are the long-term rates for atmospheric corrosion of structural steel.

Table 6. ISO Atmospheric Corrosion Category Rates

ISO Category	Steel Corrosion Rate (in/yr)
Very Low	$< 3.9 \times 10^{-6}$
Low	3.9×10^{-6} - 5.9×10^{-5}
Medium	5.9×10^{-5} - 2.4×10^{-4}
High	2.4×10^{-4} - 7.9×10^{-4}
Very High	$> 7.9 \times 10^{-4}$

The cross section loss at each weld toe is shown below in Table 7 and Table 8. 'Failure' denotes the weld toe at which the specimen failed, while 'Remaining' is the opposite weld toe of the specimen which had not failed during testing. The measurement listed under 'Failure' or 'Remaining' is the thickness lost during the corrosion-fatigue process given as a percentage of the original thickness. The 'Days' column is the amount of time the specimen was exposed to the corrosion solution.

Since all the corrosion-fatigue specimens have failed beyond the lower bound limit for Category E design life, if one were to assume that the specimens served the full AASHTO bridge design life of 75 years, the resulting ISO (1992) corrosion category for each weld toe is shown in the 'Corrosion Category' column. This 'Corrosion Category' relates the accelerated corrosion rate that the corrosion-fatigue specimens experienced to the long-term corrosion rate bridge members could be expected to experience during service life. For example, all specimens of the '2.5%-7 Day' group would correspond to the complete service life of a full size bridge member, of similar geometry, located in a 'High' ISO atmospheric corrosion category environment.

Table 7. '7 Day' Corrosion Results

Specimen	'Failure'	'Remaining'	Days	Corrosion Category
5 - 1	20%	24%	112	Medium
5 - 2	22%	18%	105	Medium
5 - 3	20%	28%	154	Medium
5 - 4	31%	33%	224	High
2.5 - 1	38%	42%	266	High
2.5 - 2	45%	48%	287	High
2.5 - 3	41%	49%	336	High
2.5 - 4	40%	38%	371	High

Table 8. '3.5 Day' Corrosion Results

Specimen	'Failure'	'Remaining'	Days	Corrosion Category
5 - 1	7%	8%	52	Low
5 - 2	1%	2%	38	Low
5 - 3	4%	4%	69	Low
5 - 4	26%	30%	188	Medium
2.5 - 1	18%	19%	97	Medium
2.5 - 2	38%	37%	181	High
2.5 - 3	35%	30%	188	High
2.5 - 4	23%	22%	174	Medium
1 - 1	51%	64%	307	High
1 - 2	52%	57%	311	High
1 - 3	52%	60%	279	High
1 - 4	58%	56%	276	High
0.5 - 1	62%	63%	283	High
0.5 - 2	72%	70%	300	High
0.5 - 3	59%	67%	279	High
0.5 - 4	71%	65%	290	High

The cross section loss measurements were taken at approximately 0.2 inches away from the weld toe at the center of the base metal. This location was chosen in order to rule out an artificially thin measurement due to material necking, which occurs during failure. Measurements were taken using a digital Mitutoyo micrometer with 0.050 inch diameter tips.

In addition to the measurements taken at the weld toe of each specimen, two coupons from a leftover section base metal ‘A’ were used to approximate the corrosion rate. The mill scale on each was removed to approximate the conditions around the weld toe where the mill scale was damaged during the welding processs, as well as to provide a uniform surface for precise and consistent measurements. Each coupon was then carefully measured and weighed. After their respective exposure periods, each coupon was removed, cleaned with a nylon brush and fine steel wool, and measured. The results can be seen in Figure 28 and Figure 29.

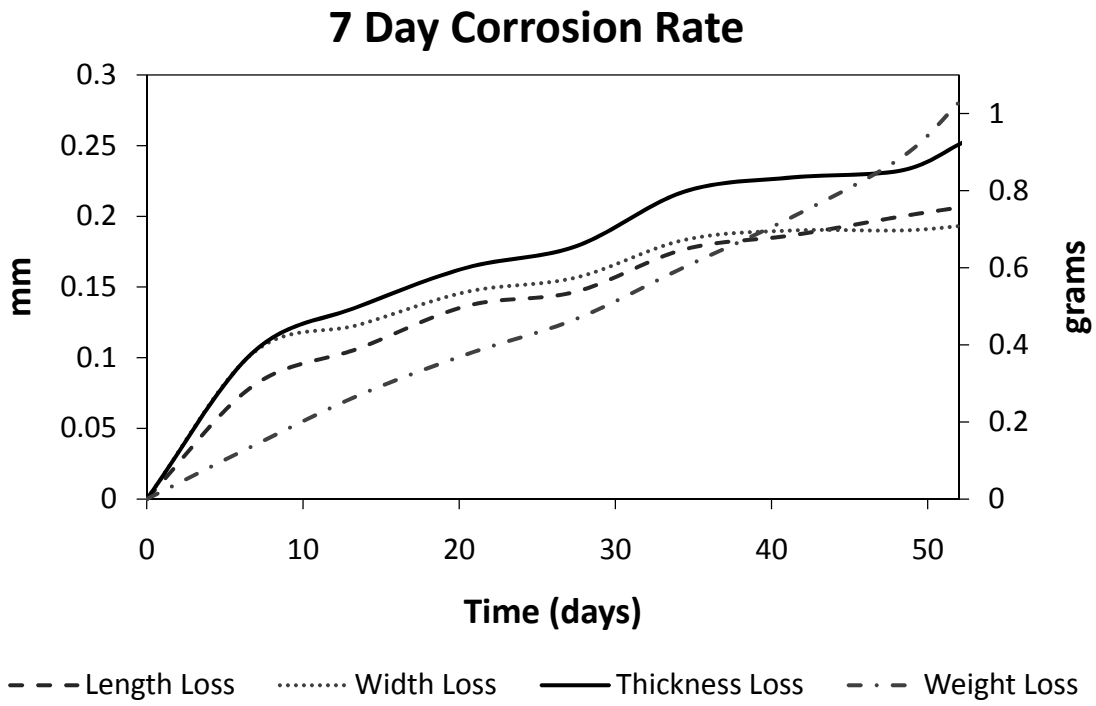

Figure 28. 7 Day Corrosion Rate

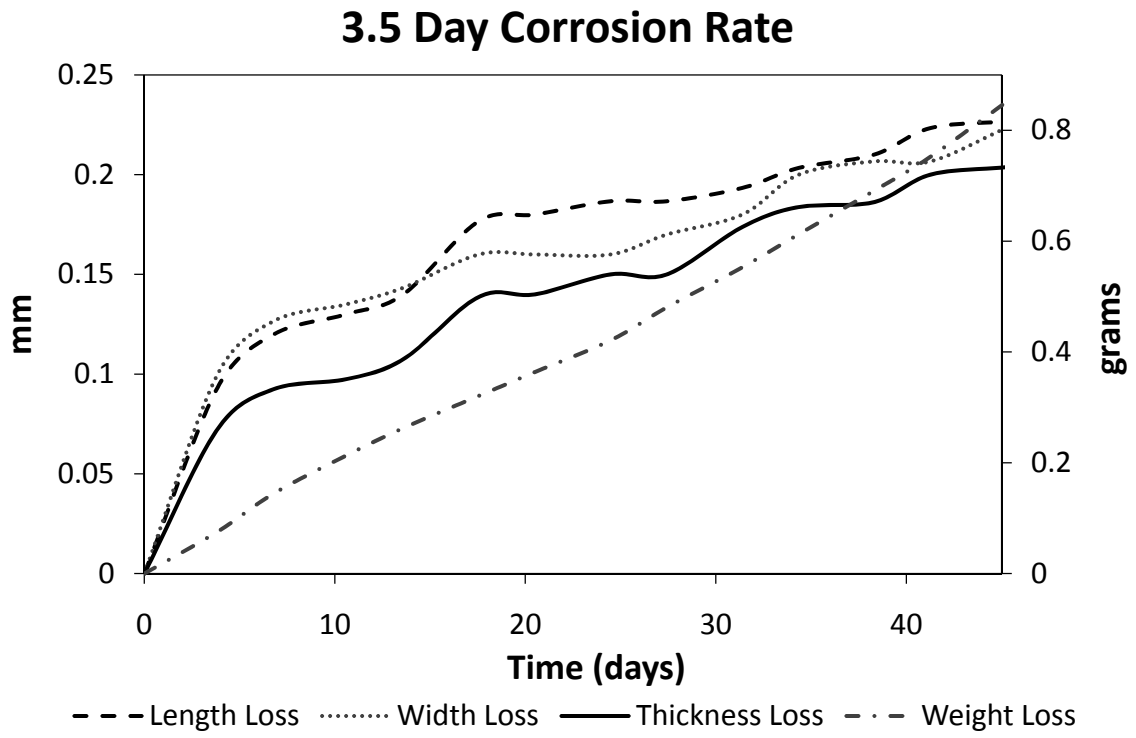

Figure 29. 3.5 Day Corrosion Rate

These coupon results can only serve as a reference for the corrosion rates experienced by the corrosion-fatigue test specimens. Since the corrosion coupons were not loaded and were smaller than the corrosion-fatigue specimens, there will inherently be some variation in the coupon corrosion rates as compared to that of the corrosion-fatigue specimens.

Although the extent of corrosion damage on each corrosion-fatigue specimen varied, Figure 30 shows how aggressive the corrosion process was as the silhouette of the remaining portion of weld toe can be seen. Figure 31 shows that the corrosion process has nearly eaten through to the root of the weld. In fact, the stiffener shown in

Figure 31 fell off when liquid nitrogen was used to fracture the remaining weld toe of the corrosion-fatigue specimen, as previously discussed; the result can be seen in Figure 32.

Figure 30. Corrosion Damage at Stiffener Termination

Figure 31. Corrosion Damage at Root of Weld

Figure 32. Advanced Corrosion led to Fracture at Weld

The corrosion results from this research are in line with the findings of Culp and Tinklenberg (1980). Table 1 shows that the weld metal has a rich chemical composition, which is similar to that of ASTM A588 weathering steel, yet Figure 30-Figure 32 show that the weld region corroded as quickly as the base metal. Since it is known that the field weathering behavior of A588 steel is not as corrosion resistant as initially thought, the findings of this research will be applicable to carbon steel, high strength low-alloy steel and weathering steels susceptible to salt contamination (Culp & Tinklenberg, 1980).

4.3 Corrosion Prior to Fatigue Loading

The results of the three pre-corroded specimens that were exposed to the corrosive environment for 376 days without experiencing any fatigue loading, are shown below in Table 9 and Figure 33. Prior to their fatigue testing, the three pre-corroded

specimens were measured to determine the approximate amount of cross sectional area lost, and thickness lost at the center of the base plate. All losses are given as percentages of original dimensions. Figure 34 shows the reduced cross section of the base plate due to the corrosion process; the white dotted line represents the original section outline.

Table 9. Pre-Corroded Specimens

Specimen	Area Loss at Failure Section	Thickness Loss at Failure Section	Fatigue Life
X-1	44%	44%	64,147
X-2	48%	47%	76,559
X-3	51%	47%	1,252

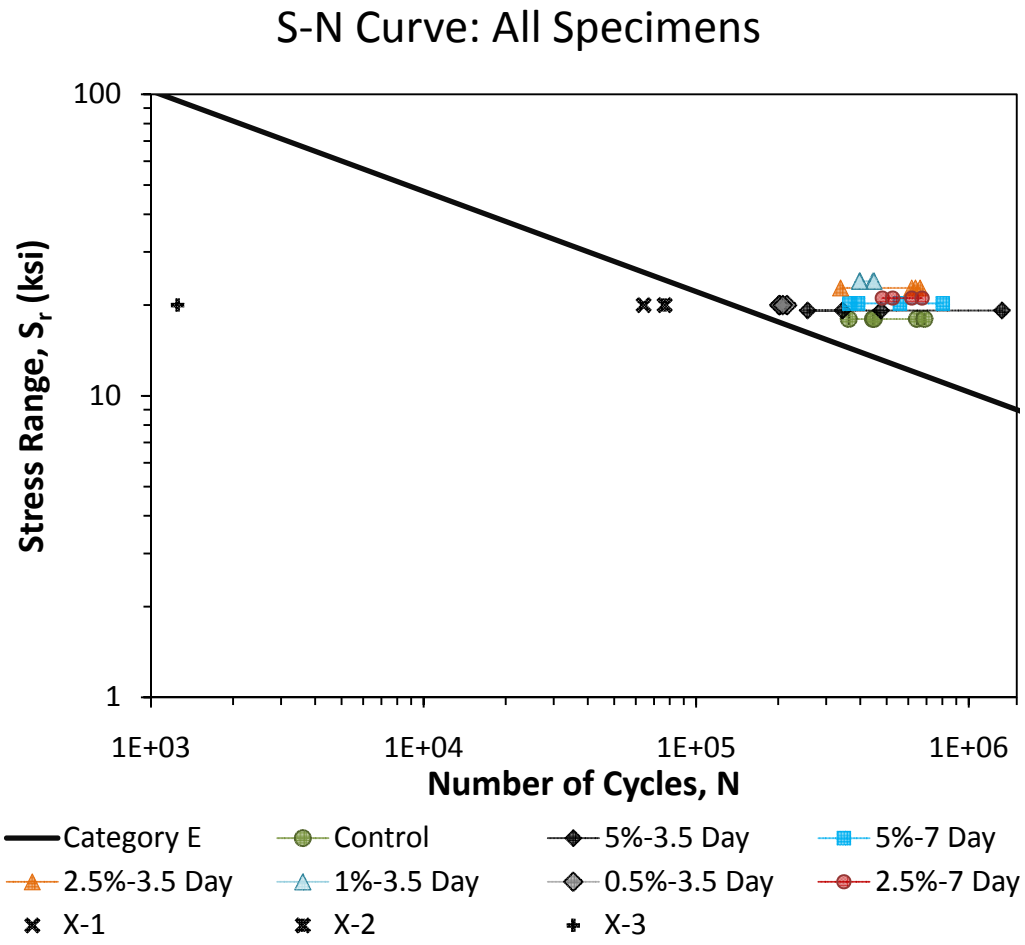

Figure 33. S-N Curve for Pre-Corroded & Corrosion-Fatigue Specimens

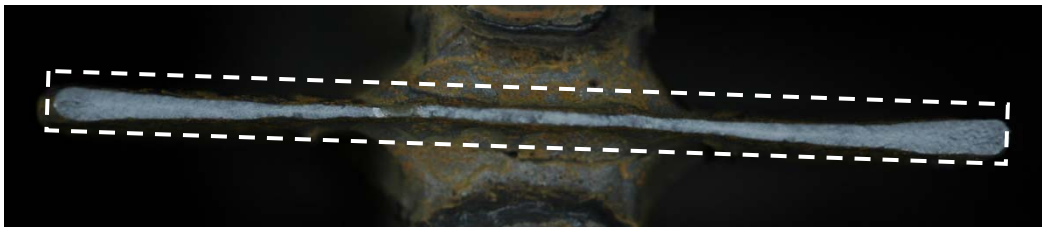

Figure 34. Reduced Cross Section

These results coincide with the findings of Albrecht et al. (1980; 1983) that weathering prior to fatigue cycling can reduce the fatigue life. By pre-corroding the specimens prior to any fatigue loading, the location of the most severe stress concentrations transition from being in the weld region to the most severe case of rust pitting. This is true for both weathering and non-weathering steels alike. For non-weathering steel, the net area is also reduced locally (Ref. Table 7 & Table 9) which causes a reduction in fatigue life.

By comparing the fatigue lives of the pre-corroded specimens with the fatigue lives of corrosion-fatigue specimens suffering similar cross section loss, it is evident that the interaction between simultaneous corrosion and cyclic loading improves fatigue life. This is because corrosion-fatigue specimens, which underwent simultaneous corrosion and fatigue loading, had much longer fatigue lives with as much, if not more, cross section loss than the pre-corroded specimens.

Although it is not captured in this study due to the small specimen geometry, if large scale specimens, composed of non-weathering steel, are allowed to weather prior to any fatigue loading, localized rust pitting and crevice corrosion may not create a sufficiently large stress concentration to limit the fatigue life. Since the stress concentration around a hole is less severe than the stress concentrations of Category E details, the fatigue life could be extended. Large scale specimens allow for force redistribution as the corrosion and fatigue mechanisms progress.

Since it is not common practice to construct a steel bridge on site and let it weather for years or even decades prior to it experiencing any cyclical loading, these results should not be reason to change the provisions regarding the design of fatigue life of welded sections. This only shows that a flawed testing methodology can produce results which may be misconstrued and lead to design provisions that may unnecessarily have a detrimental influence on future design.

5. LINEAR ELASTIC FRACTURE MECHANICS

By using linear elastic fracture mechanics, it is possible to compare the early incremental crack propagation rate to the corrosion rate. The flaws residing in a weld can be generalized as a semi-elliptical surface flaw as depicted in Figure 35 (Irwin, 1962).

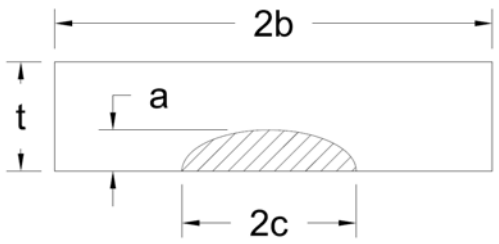

Figure 35. Elliptical Surface Crack

Although the idealized crack begins as a semi-ellipse, the ratio of the depth component (a) to the width component (2c) does not remain constant, due to the localized stress at the crack tip in the minor axis direction being larger than the localized stress in the major axis direction (Hertzberg, 1996). Smith and Smith (1983) observed that regardless of the initial ratio of the semi-elliptical depth to width, during stable growth the ratio converged to a shape "slightly shallower than semi-circular." Due to the complexity required to accurately model the entire life cycle, only the initial stage of crack propagation will be analyzed so we can neglect the differential growth rates of the

separate axes and assume that their ratio remains constant. By the time the crack reaches thru-thickness, the vast majority of the fatigue life has been exhausted. Hirt and Fisher (1973) noted that 75% of the crack growth life was spent propagating from the initial phase to a visible crack.

From Figure 26, Figure 27 and Figure 36, it is evident that the assumption of the crack shape being semi-elliptical is accurate.

Figure 36. Elliptical Crack Growth

Crack growth is defined by the Paris power law (Paris & Erdogan, 1963), which has the following form:

$$\frac{da}{dN} = C(\Delta K)^n$$

where C and n are constants taken to be $2x10^{-10}$ and 3.0, respectively, based on the average crack growth rate of structural steel (Hirt & Fisher, 1973). This equation relates the crack growth rate, da/dN (in/cycle), to the range in the stress intensity factor, ΔK

(ksi√in). The stress intensity factor is a quantitative description of the severity caused in the local stress field by a flaw. It is calculated using the following equation (Tada, Paris, & Irwin, 2000; Maddox, 1974; Albrecht & Yamada, 1978):

$$\Delta K = S_r \cdot \sqrt{\pi a} \cdot f(g)$$

where S_r is the nominal stress range (ksi) applied remotely in relation to the crack location, a is the crack depth (in) as seen in Figure 35, and f(g) is a generalized term for a correction factor which accounts for specific boundary conditions, non-uniform stress distributions, free surfaces, etc. Tada et al. (2000) has numerous solutions for various crack and specimen geometries and loading configurations.

The generalized term for correction based on specific specimen and crack geometry, f(g), is a product of the applicable correction factors, and is always greater than one. For conditions of this experiment, the correction factors are the following four: free surface correction factor, finite width correction factor, elliptical shape correction factor, and stress gradient correction factor.

$$f(g) = F_s \cdot F_w \cdot F_e \cdot F_g$$

For the assumed semi-elliptical crack geometry, a free surface correction factor, F_s, must be accounted for using the following equation (Tada, Paris, & Irwin, 2000):

$$F_s = 1.211 - 0.186\sqrt{\frac{a}{c}}$$

The finite width of the specimen is considered by the finite width correction factor, F_w (Tada, Paris, & Irwin, 2000):

$$F_w = \sqrt{\frac{2b}{\pi a}\tan\frac{\pi a}{2b}}$$

Since we are considering the initial stages of fatigue life, $F_w \cong 1$.

The elliptical crack shape correction factor, F_e, is the inverse of the complete elliptical integral of the second kind evaluated at the desired location (Irwin, 1962).

$$F_e = \frac{1}{\int_0^{\pi/2}[1 - \left(\frac{c^2 - a^2}{c^2}\right)\sin^2\theta]^{1/2}d\theta}$$

The stress gradient correction factor, F_g, for a transverse fillet weld is of the following form (Zettlemoyer & Fisher, 1977):

$$F_g = \frac{K_{tm}}{1 + 6.789(a/t)^{0.4348}}$$

where K_{tm} is the stress concentration factor for the toe of the weld.

By assuming that the initial semi-elliptical surface flaw has a depth, a_i, between 0.003-0.03 inches, the expected crack growth rates for each fatigue loading interval can be seen in Table 10 (Smith & Smith, 1983). These results were calculated by using the previously discussed correction factors and using numerical integration to determine the crack growth rates. While a nominal ratio of crack depth to width of 0.45 was chosen, in reality this ratio will vary. As previously mentioned, the initial semi-elliptical flaw shape will approach that of a slightly shallow semi-circle.

Table 10. LEFM Crack Growth Rates

Interval Cycle Count (N)	a_i (in)	$a_i/2c$	a_f (in)	$(da/dN)_{avg}$ (in/cyc)
26,000	0.003	0.45	0.0128	3.77E-07
	0.030	0.45	0.0883	2.24E-06
13,000	0.003	0.45	0.0061	2.38E-07
	0.030	0.45	0.0561	2.01E-06
5,200	0.003	0.45	0.0040	1.92E-07
	0.030	0.45	0.0397	1.87E-06
2,600	0.003	0.45	0.0035	1.92E-07
	0.030	0.45	0.0347	1.81E-06

Consider the '0.5%-7 Day' group of specimens with a hypothetical initial flaw size of 0.03 inches and a corrosion rate of 8.5×10^{-5} in/day, the average corrosion rate of that specimen sub-group. Since the specimens were corroded for 7 days prior to the

beginning of the interval fatigue loading sequence the flaw size would have been reduced from its initial depth (a_i) to 0.0294 inches. After the first fatigue loading interval of 2,600 cycles the flaw would grow to 0.0340 inches. The specimen would then be corroded for an additional 7 days, after which the flaw would be reduced to a depth of 0.0334 inches. This process would continue resulting in an initial crack growth life seen in Figure 37.

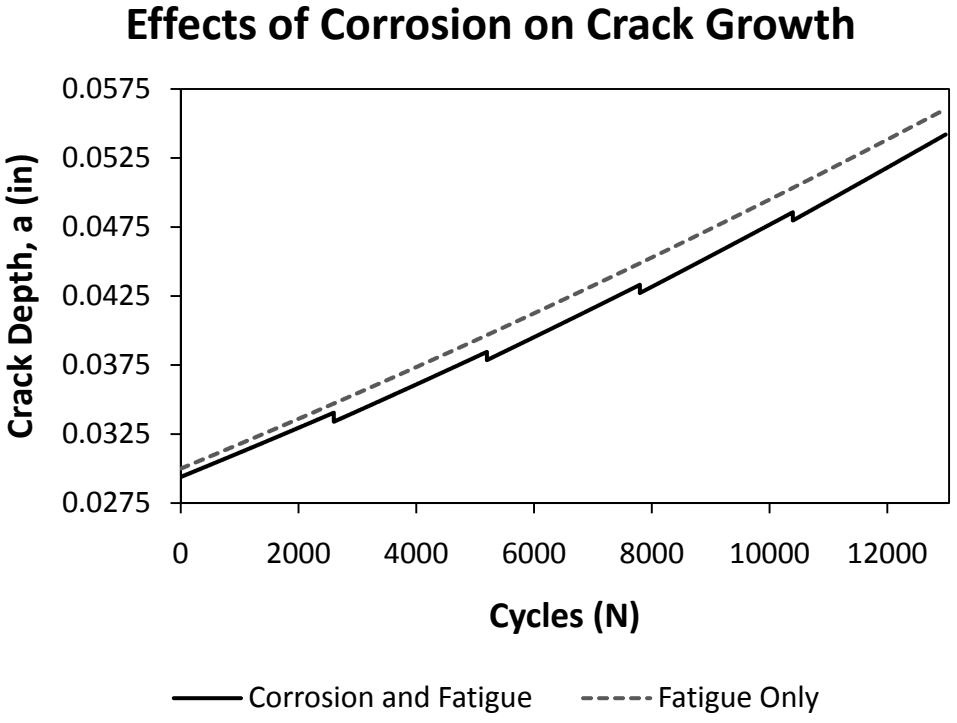

Figure 37. Crack Growth Rates

The conditions experienced during the service life of an actual bridge vary somewhat from the idealized conditions the specimens of this experiment underwent. Bridges typically see cycles on the order of tens of millions over their lifetime versus the approximately half a million cycles the control test specimens averaged. Bridges also experience much smaller stress ranges at Category E detail locations (Fisher J. , 1984). While we assumed a maximum initial flaw size depth of 0.03 inches to be our worst case, this assumption would not change as the specimen geometry changes. This means that in real bridges where a Category E detail could be the case at the transverse welded termination of a 1 inch thick cover plate over a 1.5 inch thick flange. This translates to a much smaller stress range intensity factor. Since the corrosion process is continual as is the loading rate, the resulting crack growth curve would become more horizontal than the curves in Figure 37.

It is important to recall that numerous researchers have expressed that the vast majority of the fatigue crack life is in the ‘initiation’ phase as opposed to the ‘propagation’ phase. The ‘initiation’ phase is responsible for shaping the defect into having a sharp crack-like tip. The sharp crack tip, and its corresponding area of plastic stress ahead of the crack tip, is responsible for crack growth predicted by the linear elastic fracture mechanics method used previously. It is during this ‘initiation’ phase that corrosion plays the biggest role in extending the fatigue life.

Based on the example, one can envision the scenario where the corrosion rate can consume a portion of the flaw if given the appropriate environment and sufficient time. While there are many variables associated with corrosion and fatigue crack propagation,

which make it difficult to accurately represent using traditional linear elastic fracture mechanics concepts, their basic relationship can be ascertained, as was just shown.

6. CONCLUSIONS

Due to the high variability associated with fatigue failures at welded joints, in addition to the variable nature of the corrosion process, definitive trends are difficult to isolate. However, the results of the present study show that corrosion does not decrease the fatigue life until over 50% of the cross section has been lost.

These results resolve the discrepancy between the conclusions of Albrecht et al. (1980; 1983; 2009) that weathering had a significant effect on the loss of fatigue life and the conclusions of Fisher et al. (1991), Barsom (1984), and Out et al. (1984) that the fatigue life could benefit from the corrosion process. For welded specimens simultaneously experiencing corrosion and fatigue, the fatigue life is governed by the flaws residing in the weld region until approximately half of the cross section is lost to the corrosion process.

Only two specimens failed below the minimum range of the control specimens, 5-2 and 2.5-1 of the '3.5 Day' group. This leads to the notion that corrosion can be beneficial to the fatigue life, as 63% of the corrosion-fatigue specimens did not fail at a weld toe which had suffered the most cross section loss due to corrosion.

As the corrosion process advances and the cross section is reduced, the dimensions of the crack responsible for fatigue failure decrease. During testing, the first specimens to fail gave ample warning time as it took many fatigue loading and corrosion intervals for the flaw to propagate into unstable growth, causing fracture. Later on as the

specimens got thinner, there was little to no warning prior to failure since the critical crack size was much smaller. Since the original maximum nominal stress (S_{max}) was half of the yield stress, as the cross section decreased to less than 50% of its original size, the stress experienced at the critical section approached, if not exceeded, the yield strength of the material. Due to the observed behavior, it is suggested that once an in-service bridge has been determined to be approaching 50% local section loss around welded details that the inspection schedule be adjusted accordingly.

After failure the fatigue crack surfaces were examined under a optical microscope. Due to the aggressive corrosion process, the initial fatigue crack initiation sites were typically consumed as they corroded. It was evident however, that for the specimens that lost less than 50% of their cross section to corrosion, the fatigue cracks initiated from locations of shrinkage cracks and undercuts. All of the fatigue crack failure surfaces exhibited multiple initiation sites, which coalesced into one large crack. A small number of specimens showed that micro-cracks initiated from corrosion pits located in the stress concentrated region of the weld toe. Although corrosion pits did provide locations for fatigue micro-crack nucleation to occur, the weld defects were responsible for the controlling fatigue life.

The specimens which lost more than 50% of their original thickness to corrosion typically failed from fatigue cracks originating at corrosion pits located a distance away from the weld toe, or simply from yielding due to the increase in stress of the net area, as previously discussed. This is because the advanced corrosion rate coupled with small

fatigue loading intervals eliminated the weld defects, which controlled the fatigue lives of the other specimens.

Since Category E details contain severe stress concentrations, these findings can be extrapolated to other welded details with similar or smaller degrees of stress concentration. To extrapolate these results, the detail should experience an equal or smaller stress range, without load reversal, and constant and known corrosion and fatigue loading rates. Since welded bridge details experience smaller stress ranges than the specimens of this experiment, the findings could be easily applied to bridges meeting the previously mentioned criteria.

While the conclusion of this research is that the corrosion process is not detrimental to the fatigue life of welded sections until more than half of the cross section has been lost, this should not be taken as a suggestion to encourage corrosion of steel members in service. It is not suggested to remove all protective coatings and allow free corrosion potential in all environments. Similarly, it would not be recommended to remove an in-service bridge from a corrosive environment and relocate it for service in a dry, arid environment.

Consider a typical bridge of non-weathering steel, which has been in service for a considerable time period. As time has progressed it could be a reasonable assumption that the surface coating has deteriorated and is no longer providing its original corrosion protection. If this is the case, and the bridge is not suffering from severe fatigue damage, it would not be recommended that the bridge be repainted, or any other measures be

taken to limit further corrosion. If steps were taken to prevent future corrosion, they could in fact be detrimental to the fatigue life of the structure. Not only would the painting stop future corrosion and create a condition similar to which the ‘pre-corroded’ specimens experienced, but it would also limit the effectiveness of future inspections. By repainting an existing bridge, it makes detecting fatigue crack growth by means of visual inspection more difficult.

7. FURTHER INVESTIGATION

To further investigate the effects of corrosion on the fatigue life of welded details a few modifications to the testing methodology and procedure could be recommended:

1. Use full size specimens in order to better mimic the force redistribution which occurs in bridge members. Since a corrosion bath would not be feasible for a full size beam, a fogging system could be utilized to continuously spray saltwater onto the specimen during testing. With proper planning and forethought the system could be implicated so that the actuators are not exposed to the corrosive solution and the water is drained into a large reservoir which could allow the corrosion product to settle out and reduce the frequency that the solution would need to be changed.
2. Instead of a constant amplitude load function use a variable amplitude sine wave, similar to the research Fisher (1993) conducted. This would more accurately simulate the diversity of loads experienced during service.
3. Use a variety of welding techniques. Since the bridges in service have been constructed over many years and utilized different welding processes during their construction, it could be of interest to investigate their response to the corrosion process.

4. Use a variable corrosion rate. This could be implemented by using a simple random number generator in conjunction with the fogging system described above to vary the duration of the wet/dry cycles.
5. Conduct testing on specimens near to and below the stress threshold for infinite fatigue life. It is possible that the corrosion process affects the fatigue stress threshold level due to the local reduction in cross section.
6. Implement non-destructive testing (NDT) methods to establish the initial flaw size and monitor the growth during the fatigue loading. By accurately correlating the flaw size, growth rate and corrosion rate, the AWS Bridge Welding Specifications could be rewritten to fully capitalize on any benefits the corrosion process may have on fatigue life when a bridge's service environment is known.

REFERENCES

Albrecht, P., & Cheng, J.-G. (1983). "Fatigue Tests of 8-yr Weathered A588 Steel Weldment." *American Society of Civil Engineers: Journal of Structural Engineering , 109* (9), 2048-2065.

Albrecht, P., & Friedland, I. M. (1980). "Fatigue Tests of 3-yr Weathered A588 Steel Weldement." *American Society of Civil Engineers: Journal of the Structural Division , 106* (ST5), 991-1003.

Albrecht, P., & Lenwari, A. (2009). "Fatigue Strength of Weathered A588 Steel Beams." *American Society of Civil Engineers: Journal of Bridge Engineering , 14* (6), 436-443.

Albrecht, P., & Naeemi, A. H. (1984). "Performance of Weathering Steel in Bridges." *National Cooperative Highway Research Program. Washington, D.C.: Transportation Research Board.*

Albrecht, P., & Shabshab, C. (1994). "Fatigue Strength of Weathered Rolled Beam Made of A588 Steel." *ASCE: Journal of Materials in Civil Engineering , 6* (3), 407-428.

Albrecht, P., & Yamada, K. (1978). "Rapid Calculation of Stress Intensity Factors." *Journal of the Structural Division - ASCE , 104* (8), 1326-1327.

ASM. (2003). *ASM Metals Handbook.* Materials Park: ASM.

Barsom, J. (1984). "Fatigue Behavior of Weathered Steel Components." *Washington D.C.: Transportation Research Board Report 950.*

Culp, J., & Tinklenberg, G. (1980). "Interim Report on Effects of Corrosion on Bridges of Unpainted A588 Steel and Painted Steel Types." *Research Report No. R-1142. Lansing: Michigan Transportation Commission.*

Ewalds, H., & Edwards, R. (1982). "Effect of Crack Surface Corrosion Layers on Fatigue Crack Growth." *Paper presented at EFC-meeting on Low Frequency Cyclic Loading.* Milan, Italy.

Fisher, J. (1984). *Fatigue and Fracture in Steel Bridges.* New York: John Wiley & Sons.

Fisher, J. W., Frank, K. H., Hirt, M. A., & McNamee, B. M. (1970). "Effect of Weldments on the Fatigue Strength of Steel Beams." *Washington D.C.: Transportation Research Board.*

Fisher, J. W., Kaufmann, E. J., & Pense, A. W. (1998). "Effect of Corrosion on Crack Development and Fatigue Life." *Journal of the Transportation Research Board , 1624*, pp. 110-117.

Fisher, J. W., Nussbaumer, A., & Keating, P. B. (1993). "Resistance of Welded Details Under Variable Amplitude Long-Life Fatigue Loading." *Washington D.C.: Transportation Research Board.*

Fisher, J. W., Yen, B. T., & Wang, D. (1991). "Corrosion and Its Influence on Strength of Steel Bridge Members." *Washington D.C.: Transportation Research Board Record 1290.*

Fisher, J., Albrecht, P., & Yen, B. (1974). "Fatigue Strength of Steel Beams with Welded Stiffeners and Attachments." *Washington D.C.: Transportation Research Board.*

Hertzberg, R. W. (1996). *Deformation and Fracture Mechanics of Engineering Materials* (4th ed.). John Wiley & Sons.

Hirt, M., & Fisher, J. (1973). "Fatigue Crack Growth in Welded Beams." *Engineering Fracture Mechanics , 5* (2), 415-429.

Home: Report Card for America's Infrastructure. (2011, July 28). Retrieved September 5, 2011, from Report Card for America's Infrastructure: http://www.infrastructurereportcard.org/

Irwin, G. (1962, December). "Crack-Extension Force for a Part-Through Crack in a Plate." *Journal of Applied Mechanics* , 651-654.

ISO. (1992). "Corrosion of metals and alloys - Corrosivity of atmospheres - Guiding values for the corrosivity categories." Geneva.

Maddox, S. J. (1974). "Assessing the Significance of Flaws in Welds Subject to Fatigue." *Welding Journal , 52* (9), 401-409.

Out, J., Fisher, J., & Yen, B. (1984). "Fatigue Strength of Weathered and Deteriorated Riveted Members." *Second Bridge Engineering Conference* (pp. 10-20). Transportation Research Board.

Palin-Luc, T., Perez-Mora, R., Bathias, C., Dominguez, G., Paris, P. C., & Arana, J. L. (2010, July). "Fatigue Crack Initiation and Growth on a Steel in the Very High Cycle Regime with Sea Water Corrosion." *Engineering Fracture Mechanics , 77* (11), pp. 1953-1962.

Paris, P., & Erdogan, F. (1963). "A Critical Analysis of Crack Propagation Laws." *Journal of Basic Engineering , 85* (4), 528-534.

Railroad Infrastructure Investment. (2012, January 27). Retrieved from American Association of Railroads: http://www.aar.org

Sakano, M., Arai, H., & Nishimura, T. (1989). "Long Life Fatigue Behavior of Fillet Welded Joint in Corrosive Environment." *Japan Society of Civil Engineers: Structural Engineering/Earthquake Engineering , 6* (2), 365-373.

Smith, I. F., & Smith, R. A. (1983). "Fatigue Crack Growth in a Fillet Welded Joint." *Engineering Fracture Mechanics , 18* (4), 861-869.

Tada, H., Paris, P. C., & Irwin, G. R. (2000). *The Stress Analysis of Cracks Handbook* (3rd ed.). New York: American Society of Mechanical Engineers.

Vaessen, G., deBack, J., & van Leeuwen, J. (1982). "Fatigue Behavior of Welded Steel Joints in Air and Seawater." *Journal of Petroleum Technology , 34* (2), 440-446.

van Leeuwen, J. J., deBack, J., & Vaessen, G. (1980). "Constant Amplitude Fatigue Tests on Welded Steel Joints Performed in Air and Seawater." *International Conference on Steel in Marine Structures.* Paris.

Waldvogel, T. S. (1997). "Investigating the Effects of Corrosion on the Fatigue Life of Steel." *College Station: Texas A&M University.*

Zettlemoyer, N., & Fisher, J. (1977). "Stress Gradient Correction Factor for Stress Intensity at Welded Stiffeners and Cover Plates." *Welding Journal* (56), 393-398.

VITA

Name: Jack Wesley Soape

Address: Texas A&M University
Zachry Dept. of Civil Engineering
Structural & Materials Testing Laboratory
Room 140 WERC
MS-3136
College Station, Texas 77843-3136

Email Address: jacksoape@gmail.com

Education: B.S., Civil Engineering, Texas A&M University, 2010

M.S., Civil Engineering, Texas A&M University, 2012